Surface Dielectric Barrier Discharge Plasma Actuators

E. Moreau[1], A. Debien[1], N. Bénard[1], T. Jukes[2], R. Whalley[2], K.-S. Choi[2], A. Berendt[3], J. Podliński[3], J. Mizeraczyk[3]

[1] *Pprime,University of Poitiers, CNRS, ISAE-ENSMA, Téléport 2, 86962, Futuroscope, France*
[2] *Faculty of Engineering, University of Nottingham, University Park, Nottingham, NG7 2RD, UK*
[3] *Institute of Fluid Flow Machinery, Polish Academy of Sciences, Fiszera 14, 80-231 Gdansk, Poland*

Abstract

This paper presents a part of the works conducted in the Plasmaero European project (task 1.1) on surface dielectric barrier discharge actuators applied to airflow control. The study is divided into several parts. In the first part, the goal is to enhance the electric wind produced by a typical single DBD actuator by optimization of the active electrode shape. For instance, the use of a thin wire instead of a plate air-exposed electrode has shown that the body force can be increased from 65 to 97 mN/m for a power consumption of 1 W/cm. Secondly, plasma vortex generators are presented. The interaction between the spanwise-directed body force and the oncoming boundary layer is illustrated. In the third part, the interest of using threeelectrode based sliding discharges for large-scale applications is highlighted. The final part deals with multi-DBD actuators that result in an increase of the electric wind velocity up to 10.5 m/s. This has been previous limited to about 7 m/s until now.

1 Introduction

Surface dielectric barrier discharge (DBD) plasma actuators are widely investigated for their ability to manipulate airflow [1, 2]. Their main advantages are their very short response time and their low power consumption. The well-known single DBD plasma actuator is composed of two plate electrodes asymmetrically mounted on both sides of a dielectric and supplied by an ac voltage. As a sufficient voltage is applied, a discharge occurs on the air-exposed surface. An electrohydrodynamic (EHD) body force is created and momentum transfer occurs from charged particles to neutral particles, leading to an electric wind with maximum velocity up to about 6 m/s. The present paper briefly describes a part of the works performed in the task 1.1 of the Plasmaero European project. The objective of this task was to optimize and characterize DBD plasma actuators, and to develop new actuators based on various DBD designs, such as multi-electrode DBD actuators and DBD vortex generators. The experimental works have mainly consisted of characterizing the velocity and the topology of the produced flow by time-averaged and timeresolved methods, such as particle image velocimetry. Direct measurements and indirect estimations of the EHD force have also been conducted. This paper is divided into four parts. In the first part, the goal is to enhance the mechanical performances of a single DBD actuator by modification of the active electrode shape. Thin wire electrodes and serrated electrodes have been investigated. In both cases, the use of these new electrodes results in a strong modification of the discharge behaviour. By using a thin wire, the discharge becomes filament-free, whilst a serrated electrode enables streamer locations to be regulated. As a result, this should increase the induced EHD body force and the resulting electric wind. In the second part, the goal is to explore DBD plasma actuators that create streamwise vortices, like vane-type vortex generators. This is an old flow control concept which has found many applications in industry because stream wise vortices have remarkable organisation and longevity. These DBD actuators are oriented to produce a body force at some yaw angle to the oncoming flow. This increases mixing between the boundary layer and the free-stream to reenergize the near-wall region with fluid from the outer flow. In the third part, three-electrode based actuators are presented. This type of electrode configuration has been inspired by devices used to produce sliding discharges for laser applications [3]. The three-electrode based actuator is supplied by an ac high voltage, plus a dc component. Two electrodes are flush mounted on each side of a dielectric, like the single DBD device, but a second air-exposed electrode is added and supplied by a dc voltage. This results in a "sliding" of the space charge between both air-exposed electrodes. The main advantage of this discharge is that it can be used in largescale applications because the discharge extension may be increased up to the gap between both air-exposed electrodes. Finally, the fourth part deals with multi-DBD plasma actuators. There are two goals here: an enhancement of the electric wind velocity and an enlargement of the plasma surface in order to be useful for large-scale applications. Multi-DBD actuators are usually composed of several DBD in series in order to cumulate the velocity produced by every single DBD. Innovative multi-DBD designs that have been perfected during this project will be presented and discussed. Velocity higher than 10 m/s has been measured with these configurations, which is the highest induced velocity that has ever been recorded.

2 Single DBD actuators

Two active electrode shapes were tested in order to increase the body force produced by a single DBD. The effects are summarized in the following sections.

2.1 Wire active electrode

DBD actuators are composed of two electrodes asymmetrically flush mounted on each side of a dielectric plate (3 mm-thick PMMA, Figure 1). The grounded electrode (span 90 mm, width 20 mm) is insulated with an epoxy resin. A small gap of 2 mm separates the active electrode

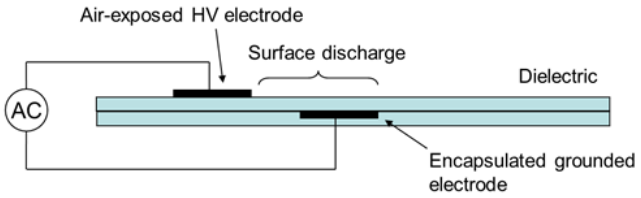


Figure 1: Schematic of a single DBD actuator

and the grounded one. For the baseline case, the active electrode is a rectangular aluminum foil (10 mm-wide, 80 μm-thick). For the new design investigated at University of Poitiers, the airexposed electrode was replaced by a thin wire in order to increase the local electric field at the vicinity of the high voltage electrode (tungsten wire with diameter of 300, 100, 50, 25 and 13 μm). The voltage waveform was sinusoidal with high voltage amplitudes from 14 to 22 kV (frequency of 1 and 1.5 kHz).

The surface dielectric barrier discharge has been experimentally investigated by electrical and optical diagnostics, electrohydrodynamic force measurements and produced electric wind characterization from timeaveraged and time-resolved measurements. Major results are going to be presented in this paper. For more details, see [4]. First, measurements of the discharge current highlighted that the discharge regime is quite different. For instance, the number of streamers that occur during the positive going-cycle decreases with the wire diameter, resulting in a filament-free regime when a 13 μm wire was used. Figure 2 shows the thrust produced by different actuators versus their electrical power consumption. The use of a thin wire electrodes results in higher thrust for a same electrical power consumption as the plate electrode. The force is larger as the wire diameter decreases. The actuator effectiveness, that corresponds to the mean produced force divided by the electrical power consumption, is increased from 0.65 mN/W to 0.97 mN/W. Then the resulting electric wind is fully modified (Figure 3). The suction effect above the surface discharge is enhanced (vertical velocity drops from -0.9 to -1.3 m/s) and the maximum horizontal velocity measured at 0.6 mm above the dielectric wall increases to about 7 m/s. Finally, the most interesting result is presented in Figure 4 that plots the time history of the electric wind at 1 mm above the wall and 5 mm downstream the active electrode. In the case of a plate-to-plate DBD, the velocity increases during the negative-going cycle (when the negative discharge ignites) and it decreases during the positive one because the streamers does not contribute efficiently to body force production (the force is negative during the positive discharge). With a wire-to-plate DBD, the velocity increases during both half cycles, with a velocity growth when the discharge occurs and a decrease when there is no discharge. Moreover, the maximum velocity is produced during the positive discharge, showing that the filament-free discharge is most efficient means of velocity production.

2.2 Serrated active electrode

DBD plasma actuators were investigated at Institute of Fluid Flow Machinery to compare the velocity of electric wind induced by a single DBD actuator with an active plate electrode having either smooth (Figure 5a) or serrated (Figure 5b) edge. In this paper, selected results are presented. For more details, see [5]. The actuators consisted of two electrodes (made of a 50 μm thick cop-

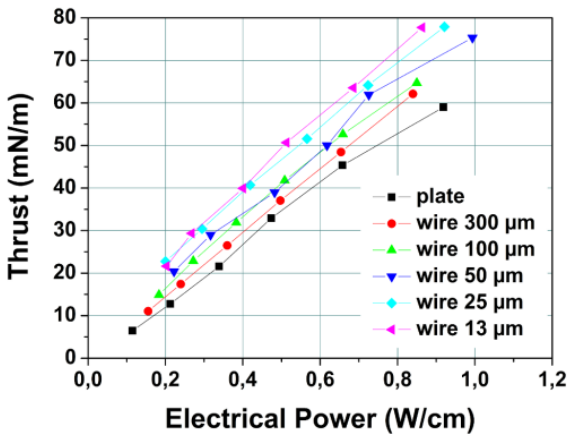


Figure 2: Discharge thrust versus electrical power (frequency = 1.5 kHz, voltages from 12 to 22 kV)

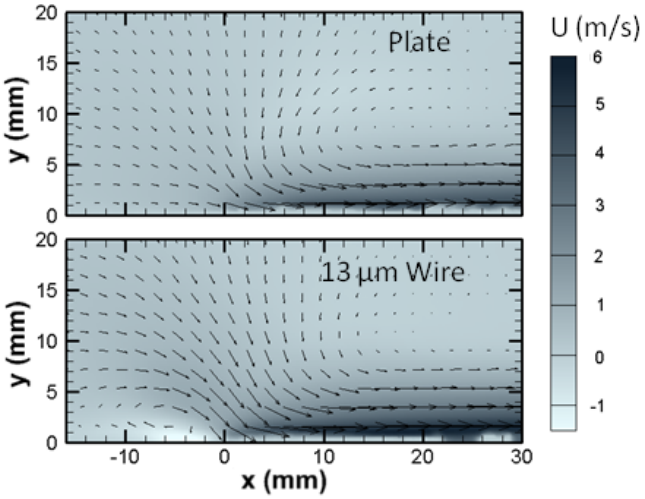


Figure 3: Velocity fields measured by PIV in stagnant air with a plate active electrode and a wire active electrode (22 kV, 1.5 kHz, scale in millimeter, edge of the active electrode at x = 0 and y = 0)

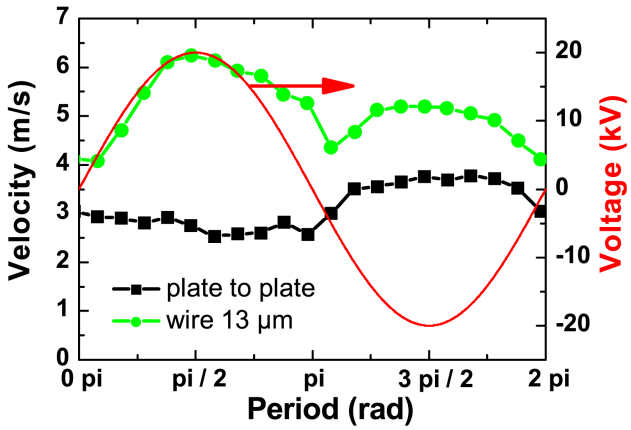


Figure 4: Velocity versus time at x = 5 mm and y = 1 mm

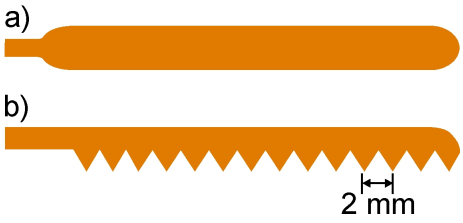


Figure 5: Top view of a smooth and serrated active electrode used in the DBD plasma actuators

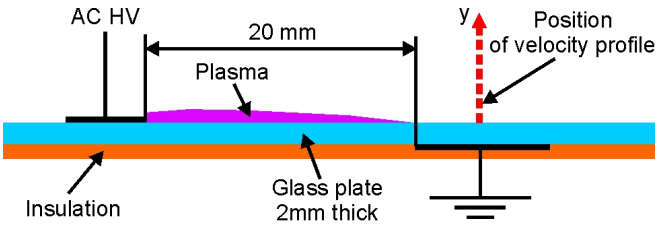


Figure 6: Schematic side view of the DBD actuator with 20 mm shift between the edges of the active and grounded electrode

per tape) flush mounted on a 2 mm thick glass plate (Figure 6). The active electrode was exposed to ambient air while the 10 mm wide grounded electrode (on the bottom side) was insulated. The width of the active electrode was equal to 6 mm and the gap between the edges of the active and grounded electrodes was 20 mm. The length of the electrodes in the span wise direction was 50 mm.

When the sine high voltage is applied to the actuators, a surface DBD is generated. The discharge generated by the actuator with serrated active electrode ignites at a lower voltage than the smooth active electrode. Moreover, the discharge starts from every saw-tooth of the serrated electrode and therefore, the plasma generated along the serrated electrode is quite homogenous (Figure 7b). When a smooth active electrode is used, the plasma is clearly non-uniform (Figure 7a).

A 2D PIV method was used to measure velocity fields of electrohydrodynamic (EHD) flow generated by the DBD actuators in quiescent air. In Figure 8, velocity profiles of the electric wind measured with both the smooth (a) and serrated (b) active electrodes are presented. These profiles are taken 25 mm downstream the edge of the active electrode (sse Figure 6). As it can be seen in Figure 8, the velocity of the EHD flow induced by the DBD actuator with serrated active electrode is higher than for the actuator with smooth active electrode in all cases. The clearest difference in flow velocity is for low voltages. For example, when the applied voltage is 22 kV (frequency 1.5 kHz), the maximum induced flow velocity obtained for the actuator with smooth electrode is

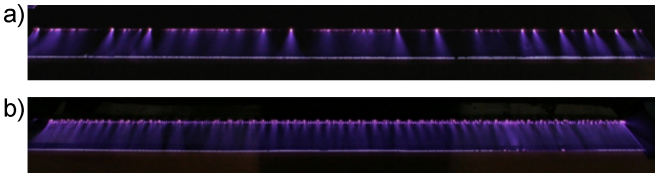


Figure 7: Images of the DBD obtained in the actuator with smooth (a) and serrated (b) active electrode. The amplitude of the applied sine-wave voltage was 26 kV, frequency 1.5 kHz

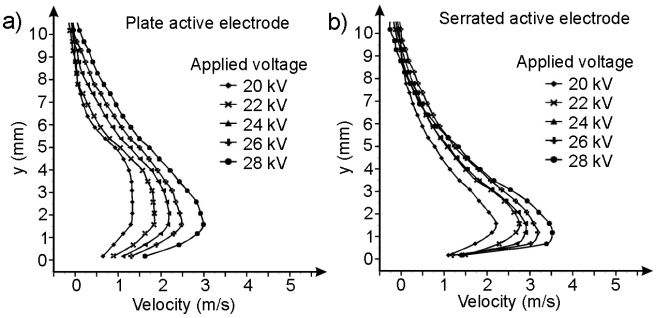


Figure 8: Velocity profiles of the EHD flow induced by the DBD actuator with smooth (a) and serrated (b) active electrode

1.8 m/s, while for the actuator with serrated electrode it reaches 2.7 m/s.

3 DBD vortex generators

The DBD vortex generator (DBD-VG) studied at University of Nottingham is a standard asymmetric DBD actuator like shown in Figure 1, oriented with component of body force perpendicular to the oncoming flow. This force vectoring interacts with the oncoming boundary layer to produce a longitudinal vortex, as depicted in Figure 9. Four key parameters affect the formation of streamwise vortex and its flow control capability: the plasma jet velocity Wp (which depends on the geometry and excitation parameters), the free-stream velocity U_∞, the electrode yaw angle β, and the DBD-VG length l. Actuators with a range of E, U_∞, β and l were studied and DBD-VGs were produced as co-rotating and counter-rotating vortex generator arrays. Further details and complete results are given in [6]. DBD-VG characterisation was carried out in a lowspeed wind tunnel over a 1 m long by 0.284 m wide smooth flat plate. The DBD-VGs were flush-mounted into the upper surface of the plate, 0.6 m from the leading edge. The free-stream velocity was set in the range $2 \leq U_\infty \leq 15 m/s$, where the local laminar boundary layer thickness at the DBD-VGs was $4.2 \leq \delta \leq 11.5$ mm. Global flow field measurements were made with timeresolved PIV in the streamwise (x-y), cross-stream (y-z), and wall-parallel (x-z) planes. Particular emphasis was placed on the vortex formation mechanisms and the growth/decay of the vortex downstream. Figure 10 shows a typical cross-stream slice through the vortex at the trailing-edge of a DBD-VG. The upper electrode is drawn in black where the electrode edge is located at the origin. Plasma forms in the region $0 < z/l < 0.05$, $y/l < 0.02$. It is clear that the DBD-VG produces a concentrated streamwise vortex. This has counterclockwise rotation in the plane of Figure 10 (black isocontour shows $\Omega_x = -100 s^{-1}$). The vortex takes less that 0.1 s to initiate (depending on U_∞) and is very stable with time. The core meandered by less than ± 2 mm whilst the plasma was on and the flow field in Figure 10 can be considered a steady-state phenomenon. When the plasma is switched off the vortex rapidly shrunk to the wall, so that longitudinal vortices can be simply turned on and off by intermittently energizing DBD-VGs. The strongest vortices were created when the DBD-VG is aligned with the flow ($\beta = 90°$), so that the DBD induced a body force predominantly in the spanwise direction. This creates a spanwise directed wall-jet flow, as can be seen in Figure 10 for $y/l < 0.05$. The upper part of this wall jet ($-\Omega_x$) rolls-up into the

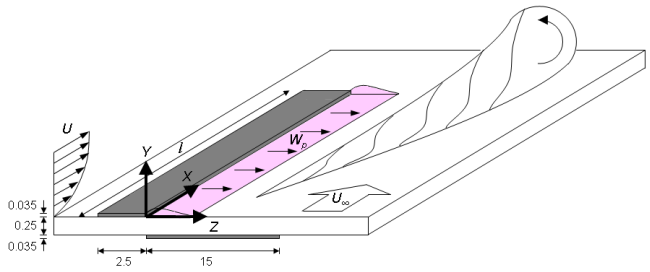


Figure 9: Schematic of a DBD-VG. Dimensions in mm

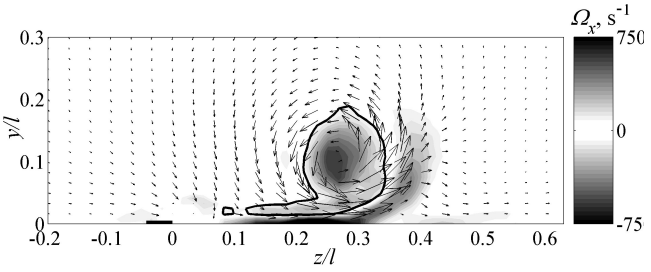


Figure 10: Ω_x with VW velocity vectors at trailing-edge of a DBD-VG. $\beta = 90°$, l = 60 mm, x = 60 mm, E = 7.5 kV_{p-p}, f = 23 kHz, U_∞ = 2.2 m/s

streamwise vortex whilst the lower part of the wall jet ($+\Omega_x$) becomes lifted from the wall on the outboard side to wrap around the core (z/l > 0.3).

Figure 11 plots the λ_2 vortex indicator, which shows the vortex is spanwise-oriented at the DBD-VG tip. This suggests that the vortex is formed as a result of lifting and twisting of spanwise vorticity ($-\Omega_z$) in the incoming boundary layer over the virtual blockage of the wall jet created by the plasma. This lifting is non-uniform across the span due to jet thickening, so the spanwise vortex filaments are increasingly lifted into region of higher U velocity with z, causing a reorientation of $-\Omega_z$ into Ω_x. This combines with $-\Omega_x$ is the outer region of the wall-jet, which supplies vorticity along the length of the DBD-VG. In addition, the DBD-VG incudes a wall-ward motion into the plasma (-V) because the plasma is a source of momentum, not mass. Thus fluid is drawn into the DBD from above to replace that accelerated laterally by the body force. The suction into the DBD is quite unlike other vortex generators and causes a dramatic thinning of the boundary layer in the downstream, as can be seen in the U iso-contours and deflection of the streamline towards the wall at z/l ≈ 0. This action occurs in addition to the cross-stream mixing of the streamwise vortex, which has proved beneficial for flow separation control [7].

4 Sliding discharges

Sliding discharge actuators are composed of two electrodes flush mounted on each side of a dielectric such as a single DBD device, plus a second air-exposed electrode supplied by a dc voltage. This results in a "sliding" of the space charge between both air-exposed electrodes [3]. These discharge are as stable as a single DBD and have the advantage that they can be used in large-scale applications because the discharge extension may be increased across the entire gap between both airexposed electrodes. However, until now, no work has investigated accurately the flow produced by these discharges compared to that induced by a single DBD. This was the objective of the

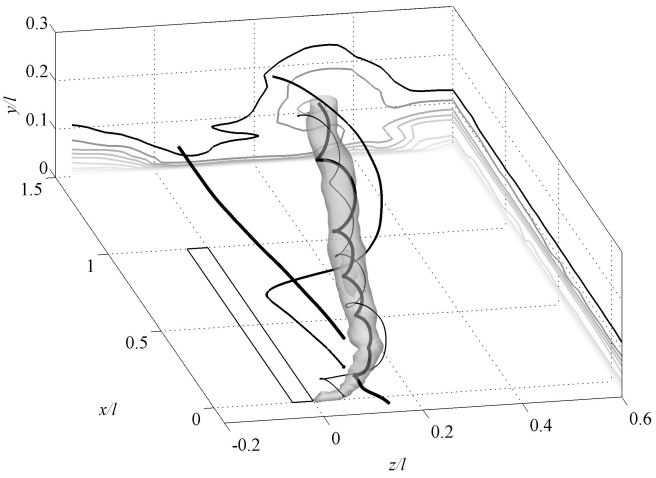


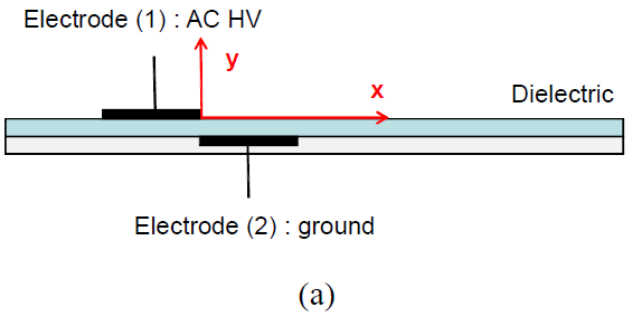
Figure 11: λ_2 iso-surface with streamlines and U isocontours ($0 \leq U/U_\infty \leq 0.9$). $\beta = 90°$, l = 60 mm, E = 7.5 kV_{p-p}, f = 23 kHz, U_∞ = 2.2 m/s. DBD-VG upper electrode in box

present study conducted at University of Poitiers. Lots of configurations have been tested. Only one is presented here. For further detail, see [8]. Figure 12 presents a schematic of a sliding discharge, with a 4-cm gap between electrodes (1) and (3). Others geometrical parameters are similar to described in Section 2.1. Figure 13 shows the velocity vector fields for a single DBD and the design of Figure 12b. One can see that the use of a third electrode, in certain conditions, can result in significant effects. First, the suction effect above and upstream the discharge is strongly increased compared to a typical single DBD. Moreover, the region where the suction is visible is strongly enlarged. Secondly, the electric wind wall jet is thickened (its height is multiplied by two). Third, the maximum electric wind velocity is slightly increased, from 4.2 to 5.5 m/s here. However, it is located 2 mm above the flat plate when it is measured at y ≈ 0.5 mm with a single DBD. This increase in velocity is due to the fact that the tangential wall jet separates from the wall at the edge of electrode (3) because a weak counter-wind is produced at this electrode. Then friction between the wall and electric wind decreases, resulting in the electric wind velocity growth.

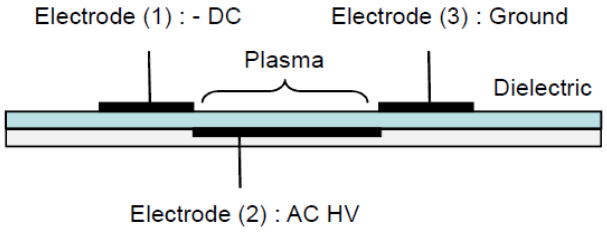
5 Multi-DBD

The goal of multi-DBD actuators is twofold: an enhancement of the electric wind velocity and an enlargement of the plasma layer in order to be useful for large-scale applications. Multi-DBD actuators are composed of several DBD in series in order to cumulate the velocity produced by every single DBD. Two innovative multi-DBD designs have been perfected during the project.

The first one, studied at University of Poitiers, consists of four successive single DBD. To take advantages of the cumulative effect, the DBD have to be close to each other, but in this case mutual interactions between electrodes can limit the velocity accumulation. This is caused by a counteracting wind caused by backdischarge from each air-exposed electrode toward the grounded electrode of the previous single DBD. In the new design proposed here, two points have been optimized compared to usual multi-DBD. First, the plate active electrodes have been replaced by thin wires (diameter of 25 μm) in order to enhance the electric wind produced by each single DBD according to the results presented previously

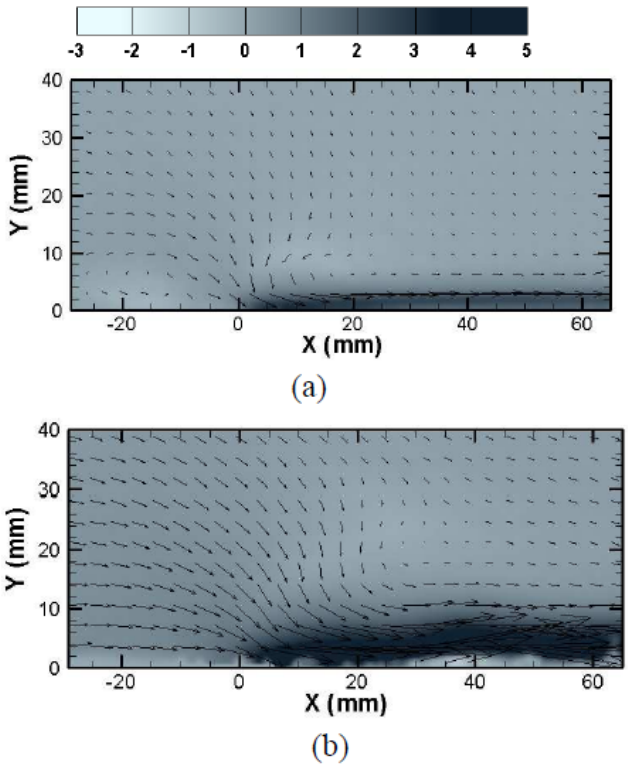


(a)



(b)

Figure 12: Sketch of a single DBD (a) and a sliding discharge (b)



(a)

(b)

Figure 13: Velocity vector fields measured for a single DBD with V_{AC} = 24 kV (a) and a sliding discharge with V_{AC} = 24 kV, V_{DC} = -24 kV (b)

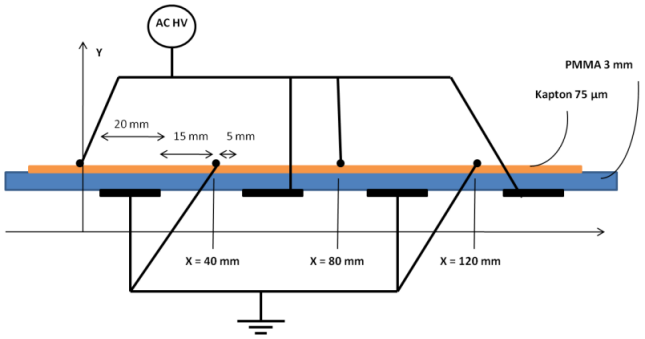


Figure 14: Sketch of the multi-DBD actuator based on four single wire-to-plate DBD

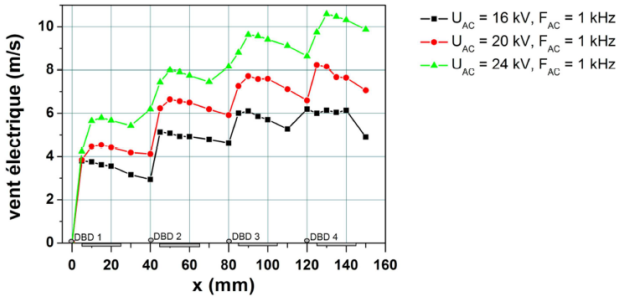


Figure 15: Horizontal velocity profiles measured 0.6 mm above a multi-DBD actuator for V_{AC} = 16, 20 and 24 kV)

in Section 2.1. Secondly, interaction between successive DBD has been cancelled by alternating the HV electrode and the grounded one, from one DBD to the successive one (see Figure 14). In such conditions, velocity measurements have been conducted with a Pitot tube. For instance, Figure 15 presents horizontal velocity profiles measured 0.6 mm above the wall, from x = 0 (position of the first wire HV electrode) to x = 145 mm (25 mm downstream the right edge of the last grounded electrode) for three different voltages. From x = 0 to about 15 mm, the velocity increases from zero to 6 m/s for 24 kV and then decreases because there is no EHD force downstream the plasma extension. Then each successive single DBD add velocity that cumulates up to 10.5 m/s downstream the last single DBD, when voltage equal to 24 kV.

The second multi-DBD actuator presented in this section consists of three successive single DBD sets with two inter-electrodes at floating potential placed between them (Figure 16). This new design has been proposed by the Institute of Fluid Flow Machinery. The grounded electrodes and the floating inter-electrodes are exposed to ambient air. The grounded electrodes are serrated (similar to that presented in Figure 5b) while the floating inter-electrodes consist of a series of separated sawteeth. The grounded and floating electrodes are partially insulated, as presented in Figure 16. The high voltage plate electrodes are on the bottom side of the actuator. They are insulated with Kapton tape. The floating electrodes are so placed over the high voltage electrodes that only their saw tips stuck out 1 mm downstream from the edge of the high voltage electrodes. Such an arrangement reduces mutual interactions between successive single DBD sets and allow us to decrease the spacing between them. Moreover, additional DBDs are generated between the floating inter-electrodes and the grounded electrodes. The flow induced by these addi-

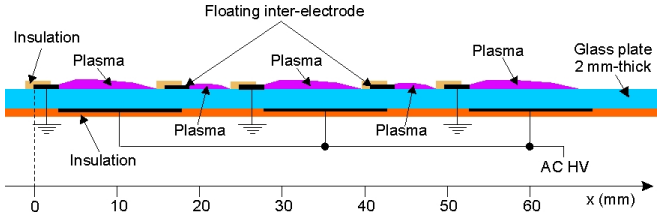


Figure 16: Schematic side view of the multi-DBD actuator with floating inter-electrodes

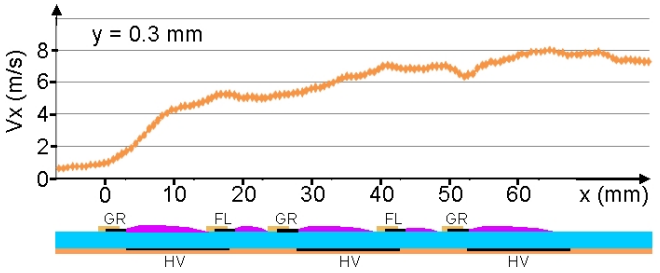


Figure 17: The horizontal time-averaged velocity profile taken 0.3 mm above actuator surface. The applied voltage 26 kV, the frequency 1.5 kHz

tional DBDs interacts coherently with the flow produced by the DBDs from grounded active electrodes, enhancing the total induced airflow. For more details see [9]. A 2D PIV system was used to characterize the total induced flow. An example of time-averaged horizontal velocity profile taken 0.3 mm above the dielectric surface is presented in Figure 17. In this case the voltage amplitude is equal to 26 kV and the frequency is set to 1.5 kHz. It can be observed that the induced airflow is almost continuously accelerated by the successive DBDs (placed close one to each other) comprising the multi-DBD actuator. The counteracting between successive DBD sets is not observed. The maximum velocity is equal to 8 m/s (just after the last grounded electrode). However, the produced velocity can be increased by increasing the ac frequency. At a frequency of 2.35 kHz, the maximum velocity was 10.1 m/s.

6 Conclusion

The works conducted in Plasmaero European project task 1.1 allowed us to investigate innovative plasma actuator designs. The body force induced by single DBD has been enhanced. Velocity above 10 m/s has been reached with both multi-DBD actuators. It is the highest velocity that has ever been measured in the case of a surface discharges. DBD-VGs have also been characterized. All of these actuators have been used for flow control applications in subsequent Plasmaero work packages.

Acknowledgments

The work has been carried out as a part of PlasmAero program with funding from the European Community's Seventh Framework Programme FP7/2007-2013 under grant agreement nr. 234201.

References

[1] E. Moreau, 2007, *Airflow Control by Non-Thermal Plasma Actuators,* Journal of Physics D: Applied Physics, Vol. 40, pp. 605-636.

[2] N. Bénard, E. Moreau, 2012, *EHD Force and Electric Wind Produced by Plasma Actuators Used for Airflow Control*, 6th AIAA Flow Control Conference, paper AIAA-2012-3136.

[3] E. Moreau, R. Sosa, G. Artana, 2008, *Electric wind produced by surface plasma actuators: a new dielectric barrier discharge based on a three-electrode geometry*, J. Phys. D: Appl. Phys., 41, 115204 .

[4] A. Debien, N. Bénard, E. Moreau, 2012, *Streamer inhibition for improving force and electric wind produced by DBD actuators,* J. Phys. D: Appl. Phys. 45, 215201.

[5] A. Berendt, J. Podliński, J. Mizeraczyk, 2011, *Comparison of airflow patterns produced by DBD actuators with smooth and saw-like electrode,* J. Phys.: Conf. Series, 301, 012018

[6] T. N. Jukes & K.-S. Choi, 2012, *Dielectric-Barrier-Discharge Vortex Generators: Characterisation and Optimisation for Flow Separation Control,* Exp. Fluids, 52, 329-345.

[7] T. Jukes, T. Segawa & H. Furutani, 2012, *Flow Control on a NACA 4418 Using Dielectric Barrier Discharge Vortex Generators,* AIAA-2012-1139 and accepted for publication in AIAA J.

[8] A. Debien, R Sosa, N. Benard, E. Moreau, 2011, *Electric wind produced by sliding discharges*, Proc. ISNPEDADM, Nov. Nouméa, France.

[9] A. Berendt, J. Podliński, J. Mizeraczyk, 2011, *Elongated DBD with floating interelectrodes for actuators,* Eur. Phys. J. Appl. Phys., 55, 13804.